Life-Cycle of Structures and Infrastructure Systems – Biondini & Frangopol (Eds)

Impact of as-recorded mainshock-aftershock excitations on seismic fragility of corrosion-damaged RC frames

Ebrahim Afsar Dizaj
Department of Civil Engineering, Azarbaijan Shahid Madani University, Tabriz, Iran

Mohammad Reza Salami
School of Engineering and the Built Environment, Birmingham City University, UK

Mohammad Mehdi Kashani
Faculty of Engineering and Physical Sciences, University of Southampton, Southampton, UK

ABSTRACT: The experience from the past seismic events shows that the accumulated damage induced by the previous earthquakes increases the vulnerability of Reinforced Concrete (RC) structures. Moreover, RC structures constructed in aggressive environments such as those located in the coastal area suffer from the ageing and degradation phenomena. Therefore, the concurrent influence of successive seismic hazards and corrosion-induced degradation might result in undesired seismic failure of these RC structures. From this perspective, this paper investigates the seismic performance of RC frames affected by chloride-induced corrosion of reinforcements subject to as-recorded (real) mainshock-aftershock excitations. To this end, a prototype RC frame is analysed under real mainshock-aftershock ground motions at different times since corrosion initiation. First, a suite of mainshock-aftershock records is selected from a unique database using the Conditional Mean Spectrum (CMS) methodology. Then, an advanced numerical model capable of tracking the low-cycle fatigue degradation and inelastic buckling of reinforcements is used to simulate the nonlinear dynamic behaviour of the studied frames with different levels of corrosion. Finally, the seismic performance and fragility of the considered structures are evaluated using the outputs of nonlinear static and incremental dynamic analyses. The results show that the vulnerability of corroded reinforced concrete frames is significantly increased under successive earthquake events. Moreover, the results of this paper show that the probability of failure of corrosion-damaged RC frames depends crucially on the magnitude of the aftershocks.

1 INTRODUCTION

The past decade witnessed several disastrous sequential earthquakes globally (Jeon et al. 2015, Raghunandan et al. 2015, Salami et al. 2019). The experience of past earthquakes shows that civil engineering structures are more vulnerable under multiple earthquake events than a single excitation.The consequence of such earthquake chains is significant damage/collapse of RC structures (Manafpour & Moghaddam 2019). Consequently, investigating the seismic performance of RC structures subject to mainshock-aftershock sequences has received considerable attention during the last decades. The outcome of these studies shows that the accumulated damage during the mainshock (MS) event significantly affects the probability of failure of structures under the second event, i.e., aftershock (AS) (Goda & Taylor 2012, Iervolino et al. 2020, Hosseinpour & Abdelnaby 2017, Salami et al. 2021).

RC structures are generally exposed to multiple stressors in their lifetime. Among the several degradation mechanisms, the chloride-induced corrosion of reinforcements has been classified as

DOI: 10.1201/9781003323020-410

one of the leading causes of the premature collapse of several RC structures/infrastructures (Afsar Dizaj & Kashani 2020, Afsar Dizaj et al. 2021, Cui et al. 2019, Panchireddi & Ghosh 2019). Several researchers have investigated the adverse influence of corrosion-induced damage on the structural performance of RC structures (Apostolopoulos & Papadakis 2008, Du et al. 2005a,b). Moreover, the seismic performance of such structures has been extensively investigated. The outcome of these studies confirms the poor seismic performance of corroded RC structures compared to their pristine status (Alipour et al. 2011, Kashani et al. 2019, Afsar Dizaj & Kashani 2022a).

The accumulated damage in the first seismic event, coupled with the increased corrosion-induced damage, can exacerbate the seismic performance of RC structures located in high seismicity regions. However, the literature review shows a significant scarcity in investigating the vulnerability of corroded RC structures subject to mainshock-aftershock excitations. To this end, this study aims to study the nonlinear dynamic behaviour and fragility of corroded RC frames subject to real (as-recorded) mainshock-aftershock ground motions. In the following sections, the details of the study are presented.

2 PROTOTYPE RC FRAME

2.1 *Structural details*

Figure 1 shows the geometry and structural details of the prototype RC frame considered here to study the combined effects of earthquake sequences and corrosion-induced degradation on the seismic fragility of RC structures. The frame is located in California, US, with harsh environmental conditions. It is designed according to the requirements of ACI 318–02 (2002) and ASCE 7–02 (2002). In Figure 1, H and B denote the depth and width of components; ρ_l is the vertical reinforcement ratio; ρ_v is the volumetric ratio of transverse reinforcements; S_h is the spacing of hoops; and ρ_{top} and ρ_{bot} are longitudinal reinforcement ratio at the top and bottom of beam section, respectively. Further information on design assumptions and details of this frame is available in (Afsar Dizaj et al. 2022).

Different corrosion statuses, including (*i*) pristine, (*ii*) slightly corroded and (*iii*) highly corroded conditions, are considered to investigate the influence of corrosion degree on the structural performance of the considered RC frame. The material and geometrical properties of the frame are updated using the mass loss ratio of rebars (ψ) in any of the corrosion statuses mentioned above. This parameter can be calculated using Equation 1 (Afsar Dizaj 2022):

$$\psi = 1 - \left(\frac{XD - 1.05 \times (1 - W/C)^{-1.64} \times t^{0.71}}{XD} \right)^2 \tag{1}$$

where X is cover thickness, D is the diameter of main bars; W/C is the water-to-cement ratio, and t is the time from corrosion initiation. In order to induce the hypothetical corrosion degrees mentioned above, t is assumed to be 0, 10, and 100 years for pristine, slightly corroded and highly corroded conditions, respectively. Further details can be found in (Afsar Dizaj 2022).

2.2 *Numerical model*

In this study, the advanced nonlinear finite element model developed in (Afsar Dizaj et al. 2018a, b) is employed to simulate the nonlinear behaviour of the case-study RC frame. Figure 2 shows the numerical model of the hypothetical RC frame. This model can simulate the inelastic buckling behaviour and low-cycle fatigue degradation of reinforcements. As Figure 2 shows, columns and beam are divided into several fibre sections in their entire length in this model. Moreover, each component is modelled using three force-based elements: a zero-length section element to simulate the slippage of reinforcement at connection adjacents, a force-based element with three integration points and another element with five

integration points. The details of this modelling technique are presented in the systematic modelling guidelines provided in (Afsar Dizaj & Kashani 2022b).

The material properties used in numerical modelling are tabulated in Table 1.

Table 1. Steel and concrete material properties.

Notation	Description	Value	Unit
f_y	yield strength of main bars	420	MPa
f_u	ultimate strength of main bars	620	MPa
f_{yh}	yield strength of hoops	300	MPa
E_s	modulus of elasticity of steel	210	GPa
f_c	compressive strength of concrete	35	MPa
ε_u	ultimate strian of main bars	0.18	-
ε_s	strain at maximum stress of hoops	0.15	-

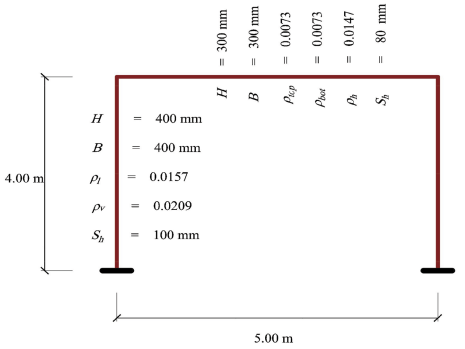

Figure 1. Structural details of the prototype RC frame.

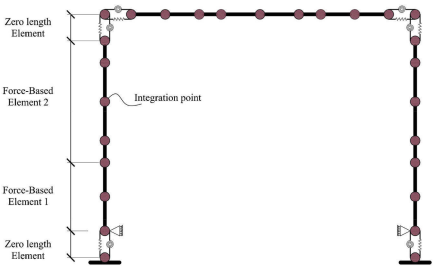

Figure 2. Finite element model of the prototype RC.

3 PUSHOVER ANALYSIS

In order to quantify the time-dependent damage limit states, nonlinear pushover analysis is carried out on the considered RC frames with different hypothetical corrosion statuses. Before conducting the pushover analysis, the material and geometrical properties of the frame are modified to incorporate corrosion-induced degradation. Moreover, the bases of the columns are assumed to be fully fixed. The P-delta effects are also included in the analyses.

Figure 3 shows the time-dependent pushover analysis results for each considered time from corrosion initiation. Results show that as the corrosion level increases, the ductility and lateral load capacity of the frame significantly decrease. The onset of bar yielding, cover concrete spalling, core concrete crushing, and bar fracture are mapped on each capacity curve. The results indicate that each of these damage limit states reaches in lower drift ratios for higher corrosion degrees. For instance, while the core cover spalling occurs at approximately 0.021 drift ratio for the slightly corroded frame, it took place at the vicinity of 0.015 drift ratio for the highly corroded frame. These time-dependent damage limit states are used in this study to develop time-dependent fragility curves.

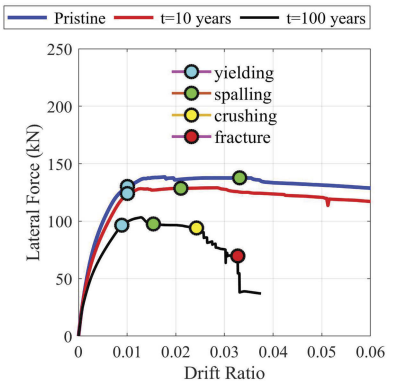

Figure 3. Time-dependent pushover analysis results.

4 MAINSHOCK-AFTERSHOCK GROUND MOTION SELECTION

The selection of aftershocks is a critical step toward conducting incremental dynamic and fragility analysis of structures. The review of previous studies shows that improper selection of mainshock-aftershock ground motions can significantly bias the expected seismic performance of RC structures (Goda 2015). Several researchers have welcomed using as-recorded MSAS ground motion records in recent years (Goda & Taylor 2012, Goda 2015). Similarly, in this study, as-recorded (real) MSAS record sequences are selected to conduct vulnerability analysis of studied RC frames with varied corrosion levels.

Here, conditional mean spectrum (CMS) methodology is used to select a sufficient number of MSAS sequences. To this end, the spectral acceleration at the first fundamental period of the frame is considered as the intensity measure (IM). Moreover, the local seismicity level and soil class of the site are taken into account. Further details about the MSAS ground motion selection are presented in (Afsar Dizaj et al. 2022). In total, forty-eight MSAS ground motion records are selected to be utilised in IDAs. Figure 4 shows the disaggregation data and spectral acceleration response of selected ground motions. The summary of the selected as-recorded MS-AS ground motion sequences is available in Afsar Dizaj et al. (2022).

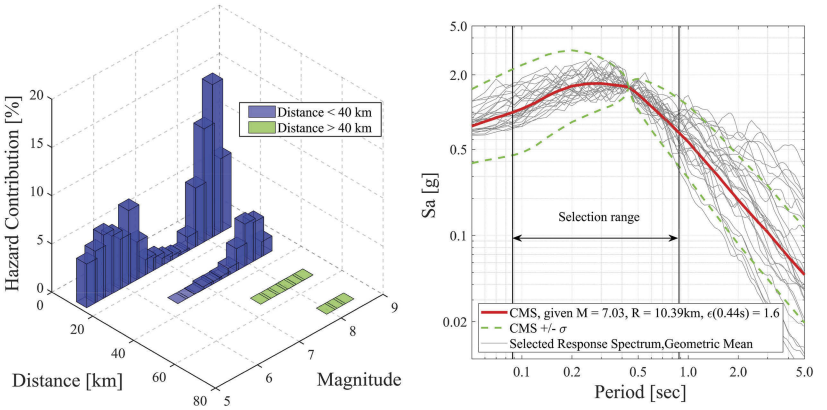

Figure 4. Selected ground motions: (a) disaggregation data, and (b) selected MSAS sequences.

5 RESULTS AND DISCUSSION

5.1 *IDA results*

Using the selected MSAS ground motion records, IDA is conducted on studied RC frames. First, the MS acceleration histories with scaled-up intensities in $Sa(T_1)$ were applied to the frames, and the structural response in terms of maximum lateral drift was recorded. Then, a 60 seconds rest time was inserted between the MS and AS records, and the assembled MSAS sequence was used as input to conduct MSAS IDAs.

Figure 5 compares the IDA results under MS event with MSAS excitation. This figure shows that for a drift ratio less than 0.025, the median MSAS IDA curves are approximately the same as MS IDA curves. However, for higher drift ratios, for a specific intensity of earthquake record, the frame experiences greater drift ratios under MSAS sequence rather than a single MS record (Figure 5a). As Figure 5b shows, a likewise trend can be seen for t=10 years. However, as Figure 5c shows, the median IDA response of severely corroded frame under MSAS sequence is approximately the same as that of MS. Such a trend in median IDA outputs can be attributed to premature material failure in higher corrosion levels. Consequently, the frame fails under the MS event before the upcoming event (i.e., AS) occurs. The results obtained in the shake table experiment of severely corrosion-damaged RC columns (Ge et al. 2020) confirm the results obtained in this study.

5.2 *Fragility curves*

In this section, the failure probability of examined frames under MS and MSAS records is investigated. To this end, the following fragility function is used:

$$P[EDP \geq DS|IM = x] = 1 - \boldsymbol{\Phi}\left(\frac{\ln(\mathrm{DS}) - \ln(\mu)}{\beta}\right) \tag{2}$$

where P[.] is the probability that the engineering demand parameter (EDP) exceeds a damage state (DS) provided that the intensity of the earthquake equals x. Here, the EDP is assumed to be the peak drift ratio. On the right side of Equation 2, Φ(.) is the lognormal distribution function with the logarithmic mean, and standard deviation of ln(μ) and β, respectively, which can be obtained using Equations 3-4:

$$\ln(\mu) = \frac{\sum_{i=1}^{n} \ln(\mathrm{EDP}_i)}{n} \tag{3}$$

$$\beta = \sqrt{\frac{\sum_{i=1}^{n} (\ln(\mathrm{EDP_i}) - \ln(\mu))^2}{n-1}} \tag{4}$$

In Equations 3-4, n is the number of records, and $\mathrm{EDP_i}$ is the peak drift ratio associated with a given value of IM for the i_{th} record.

Figure 6 shows the MS and MSAS fragility curves for all frames. Figure 6 shows that the probability of exceeding the collapse threshold under MSAS records is somewhat greater for a given IM than MS records. This indicates that the studied RC frames with varied corrosion levels are slightly more vulnerable under MSAS ground motions sequences than MS records. Therefore, it can be concluded from the results that, as observed in IDA results (Figure 5), the real MSAS records have a negligible impact on the nonlinear dynamic behaviour and fragility of corroded RC frames.

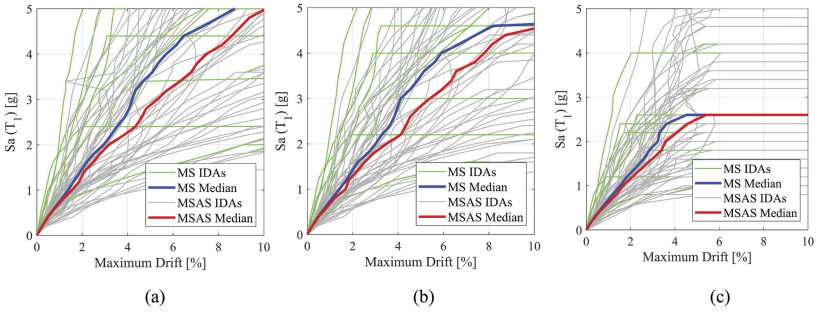

Figure 5. IDA results: (a) pristine frame, (b) t= 10 years and (c) t= 100 years.

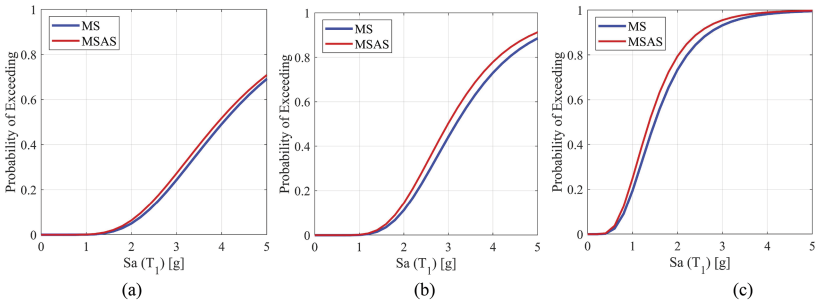

Figure 6. Fragility curves: (a) pristine frame, (b) t= 10 years and (c) t= 100 years.

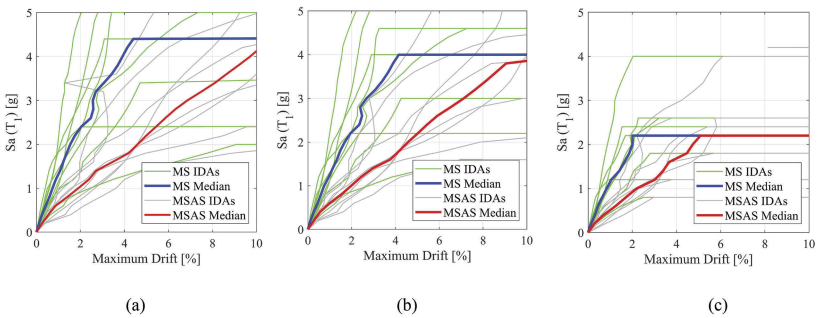

Figure 7. IDA results for records with higher AS/MS PGA ratio: (a) pristine frame, (b) t= 10 years and (c) t= 100 years.

5.3 *Impact of aftershock intensity*

The results presented in the previous section indicated that the MSAS records slightly increase the failure probability of RC frames, regardless of aftershock magnitude. In this section, the influence of aftershock to mainshock intensity ratio on nonlinear dynamic behaviour and fragility of studied RC frames is investigated. To this end, from the entire 48 selected MSAS sequences, those with aftershock PGA to mainshock PGA greater than or equal to unity are selected. There are eight ground motion records with this property. In Figure 7, presents the median IDA results of the frames under these eight records. As Figure 7 shows, under the stronger aftershock records, all the frames experience significantly higher drift ratios in all the frames. This implies that the response of a RC frame under MSAS sequence crucially depends on the intensity of the aftershock records.

Figure 8 shows the failure fragility curves under the selected MSAS sequence records with higher PGA of aftershocks to their MS. As this figure shows, the collapse probability of the pristine frame and the slightly corroded frame is not remarkably affected by the PGA ratio of

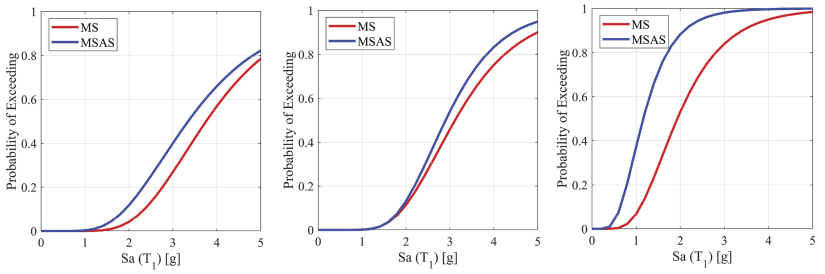

Figure 8. Fragility curves for records with higher AS/MS PGA ratio: (a) pristine frame, (b) t= 10 years and (c) t= 100 years.

aftershock to the mainshock. However, as shown in Figure 8c, the highly corrosion-damaged frame is much more fragile under the MSAS sequence than MS records. This infers that the PGA ratio of aftershock to mainshock is a critical factor in the fragility analysis of corrosion-damaged RC frames.

6 CONCLUSIONS

In this study, the seismic performance of corrosion-damaged RC frames under MSAS sequences is investigated. To this end, an advanced modelling methodology was employed to accurately simulate the nonlinear behaviour of RC frames with varied corrosion levels, including an uncorroded frame, a slightly corroded frame and a highly corroded frame. First, nonlinear pushover analysis is carried out on the studied RC frames to quantify the time-dependent seismic damage limit states. Subsequently, IDAs conducted using a suite of 48 as-recorded mainshock-aftershock ground motion records. Finallly, the fragility curves were developed using the IDA outputs for the frames under MS records and MSAS sequences.

Overall, the results show that using the real mainshock-aftershock sequences, the failure probability of corrosion-damaged frames slightly increases with respect to MS events. Notably, for the highly corroded frame, the results show that in most cases, the structure fails under the MS record before the subsequent event (i.e., aftershock) comes up. This is due to the brittle failure mode of extremely corroded RC frame due to premature failure of confinements.

Moreover, results show that the PGA ratio of aftershock to mainshock plays a critical role in the vulnerability assessment of corroded RC frames. This conclusion is drawn based on eight MSAS records with higher PGA of aftershock records, where the results showed a significantly higher failure probability of structure under MSAS records.

REFERENCES

ACI. 2002. Building code requirements for structural concrete. ACI 318-02, *American Concrete Institute*, Farmington Hills.

Afsar Dizaj, E. 2022. Modelling Strategy Impact on Structural Assessment of Deteriorated Concrete Bridge Columns. *Proceedings of the Institution of Civil Engineers-Bridge Engineering* 175 (4): 246–262. https://doi.org/10.1680/jbren.21.00003.

Afsar Dizaj, E. & Kashani, M.M. 2020. Numerical investigation of the influence of cross-sectional shape and corrosion damage on failure mechanisms of RC bridge piers under earthquake loading. *Bulletin of Earthquake Engineering* 18: 4939–4961. https://doi.org/10.1007/s10518-020-00883-3.

Afsar Dizaj, E. & Kashani, M.M. 2022a. Influence of ground motion type on nonlinear seismic behaviour and fragility of corrosion-damaged reinforced concrete bridge piers. *Bulletin of Earthquake Engineering* 20: 1489–1518. https://doi.org/10.1007/s10518-021-01297-5.

Afsar Dizaj, E. & Kashani, M.M. 2022b. Nonlinear Structural Performance and Seismic Fragility of Corroded Reinforced Concrete Structures: Modelling Guidelines. *European Journal of Environmental and Civil Engineering* 26(11): 5374–5403. https://doi.org/10.1080/19648189.2021.1896582.

Afsar Dizaj, E., Madandoust, R., Kashani, M. M. 2018a. Exploring The Impact of Chloride-Induced Corrosion on Seismic Damage Limit States and Residual Capacity of Reinforced Concrete Structures. *Structure and Infrastructure Engineering* 14(6): 714–729. http://dx.doi.org/10.1080/15732479.2017.1359631.

Afsar Dizaj, E., Madandoust, R., Kashani, M.M. 2018b. Probabilistic seismic vulnerability analysis of corroded reinforced concrete frames including spatial variability of pitting corrosion. *Soil Dynamics and Earthquake Engineering* 114: 97–112. https://doi.org/10.1016/j.soildyn.2018.07.013.

Afsar Dizaj E, Padgett J.E., Kashani, M.M. 2021. A Markov Chain-Based Model for Structural Vulnerability Assessment of Corrosion-Damaged Reinforced Concrete Bridges. *Philosophical Transactions of The Royal Society A Mathematical Physical and Engineering Sciences* 379 (2203). https://doi.org/10.1098/rsta.2020.0290.

Afsar Dizaj, E., Salami M.R., Kashani, M.M. 2022. Seismic Vulnerability Assessment of Ageing Reinforced Concrete Structures under Real Mainshock-Aftershock Ground Motions. *Structure and Infrastructure Engineering* 18(12): 1674–1690. https://doi.org/10.1080/15732479.2021.1919148.

Alipour, A., Shafei, B., Shinozuka, M. 2011. Performance evaluation of deteriorating highway bridges located in high seismic areas. *Journal of Bridge Engineering* 6: 597–611. https://doi.org/10.1061/(ASCE)BE.1943-5592.0000197.

Apostolopoulos, C.A., Papadakis, V.G. 2008. Consequences of steel corrosion on the ductility properties of reinforcement bar. *Construction and Building Materials* 22(12): 2316–2324. https://doi.org/10.1016/j.conbuildmat.2007.10.006.

ASCE-7. 2002. Minimum design loads for buildings and other structures. Structural Engineering Institute.

Cui, Z., Alipour, A., Shafei, B. 2019. Structural performance of deteriorating reinforced concrete columns under multiple earthquake events. *Engineering Structures* 191: 460–468. https://doi.org/10.1016/j.engstruct.2019.04.073.

Du, Y.G., Clark, L.A., Chan, A.H.C. 2005a. Residual capacity of corroded reinforcing bars. *Magazine of Concrete Research* 57(3): 135–147. https://doi.org/10.1680/macr.2005.57.3.135.

Du, Y.G., Clark, L.A., Chan, A.H.C. 2005b. Effect of corrosion on ductility of reinforcing bars. *Magazine of Concrete Research* 57(7): 407–419. https://doi.org/10.1680/macr.2005.57.7.407.

Ge, X., Dietz, M.S., Alexander, N.A., Kashani, M.M. 2020. Nonlinear dynamic behaviour of severely corroded reinforced concrete columns: shaking table study. *Bulletin of Earthquake Engineering* 18: 1417–1443. https://doi.org/10.1007/s10518-019-00749-3.

Goda, K., Taylor, C.A. 2012. Effects of aftershocks on peak ductility demand due to strong ground motion records from shallow crustal earthquakes. *Earthquake Engineering and Structural Dynamics* 41 (15): 2311–30. https://doi.org/10.1002/eqe.2188.

Goda, K. 2015. Record selection for aftershock incremental dynamic analysis. *Earthquake Engineering and Structural Dynamic* 44(7): 1157–1162. https://doi.org/10.1002/eqe.2513.

Hosseinpour, F. & Abdelnaby, A. E. 2017. Effect of different aspects of multiple earthquakes on the nonlinear behavior of RC structures. *Soil Dynamics and Earthquake Engineering* 92: 706–725. https://doi.org/10.1016/j.soildyn.2016.11.006.

Iervolino, I., Chioccarelli, E., Suzuki, A. 2020. Seismic damage accumulation in multiple mainshock–aftershock sequences. *Earthquake Engineering and Structural Dynamics* 49(10): 1007–1027. https://doi.org/10.1002/eqe.3275.

Kashani, M. M., Maddocks, J., & Afsar Dizaj, E. 2019. Residual capacity of corroded reinforced concrete bridge components: A state-of-the-art review. *Journal of Bridge Engineering* 24(7): 03119001. https://doi.org/10.1061/(ASCE)BE.1943-5592.0001429.

Manafpour, A.R. & Moghaddam, P.K. 2019. Performance capacity of damaged RC SDOF systems under multiple far- and near-field earthquakes. *Soil Dynamics and Earthquake Engineering* 116: 164–173. https://doi.org/10.1016/j.soildyn.2018.09.045.

Panchireddi, B., Ghosh, J. 2019. Cumulative vulnerability assessment of highway bridges considering corrosion deterioration and repeated earthquake events. *Bulletin of Earthquake Engineering* 17: 1603–1638. https://doi.org/10.1007/s10518-018-0509-3.

Raghunandan, M., Liel, A.B., Luco, N. 2015. Aftershock collapse vulnerability assessment of reinforced concrete frame structures. *Earthquake Engineering and Structural Dynamics* 44: 419–439. https://doi.org/10.1002/eqe.2478.

Salami M.R, Afsar Dizaj E, Kashani M.M. 2019. The behavior of Rectangular and Circular Reinforced Concrete Columns under Biaxial Multiple Excitation. *Computer Modeling in Engineering & Sciences* 120 (3): 677–691. https://doi.org/10.32604/cmes.2019.05666.

Salami M.R., Afsar Dizaj E., Kashani, M.M. 2021. Fragility analysis of rectangular and circular reinforced concrete columns under bidirectional multiple excitations. *Engineering Structures*, 233, 111887. https://doi.org/10.1016/j.engstruct.2021.111887